



## NUMERICAL STUDY OF VARIOUS GEOMETRIES OF BREAKWATERS FOR THE INSTALLATION OF FLOATING WIND TURBINES

Keyvan Esmaeelpour<sup>1</sup>, Rouzbeh Shafaghat<sup>1\*</sup>, Rezvan Alamian<sup>1</sup> and Rasoul Bayani<sup>1</sup>

<sup>1</sup>Department of Mechanical Engineering, BabolNoshiravani University of Technology, Babol47148-71167, Iran

\*Email: [rshafaghat@nit.ac.ir](mailto:rshafaghat@nit.ac.ir)

### Abstract:

*The everyday growing populations all over the world and the necessity of increase in consumption of fossil energies have made the human to discover new energy resources, which are clean, cheap and renewable. Wind energy is one of the renewable energy resources. Considerable wind speed has made settling of wind turbines at sea beneficial and appealing. For this purpose, choosing the appropriate plates to set up wind turbines on the surface of sea is necessary. Regarding the installation condition, by choosing suitable geometry for floating breakwaters, offshore wind turbine can be mounted on them. Suitable geometry of breakwater for multifunctional usage could be selected with analyzing and comparing pressure, force and moment produced by incoming waves. In this article, the boundary element method is implemented to solve governing differential equations by assuming potential flow. On the other hand, for promoting free surface in each time step, the Euler-Lagrangian method is employed. Finally, to find the appropriate geometry for installing the wind turbine on the breakwater, moment and wave profile next to the right and left side of breakwater body are calculated. Among simulated geometries, breakwater with trapezoid geometry which its larger base is placed in the water has more sustainability and it is the most suitable geometry for wind turbine installation.*

**Keywords:** Wind turbine, floating breakwater, boundary element method, Euler -Lagrangian method

### 1. Introduction

Using different sources like coal, natural gas, oil and nuclear energy always have been noticed in different part of the world. The important factors about these resources are their environmental hazard and limited amount, while renewable energies are limitless and non-pollutant; so, they have been considered as substitute of traditional energy resources. Wind energy is one of renewable energies; it has considerable potential for satisfying human energy demands. Wind turbines installed on lands have been used for a long time, but in recent years because of relevant sea's potential, installing wind turbines in seas have been noticed (Mostafa et al. 2012). Considerable wind energy at sea, as a result of high wind speed and having less surface roughness than lands, make this choice more appealing. Some advantages of utilizing offshore wind turbines are (Withee 2004):

- Offshore wind turbines unlike land turbines do not effect on nearby road and railroads.
- Floating wind turbines do not create visual and noise pollution as a result of distance of wind farm from shore.
- Due to the large area of seas, fertile lands are not occupied.
- Under some conditions, floating wind turbines need less maintenance than land wind turbines.

There are difficulties in installing offshore wind turbines that must be analyzed to identify appropriate condition of installation. Most important part in erecting wind turbines is providing structure stability which is possible by analyzing forces, moments and motion of the heave plate. Important hints in designing heave plates are (Fulton et al. 2007):

- The plate must bear its own weight and wind turbine connected.
- It must remain stable under any circumstances of wind and waves.
- The wind turbines should be abstained from overloading because of waves crashing to the floater.
- It must be economically feasible.

The main purpose of this research is investigating wave condition in order to evaluate system stability. Figs. 1 and 2 show two principal methods in installing offshore wind turbines.

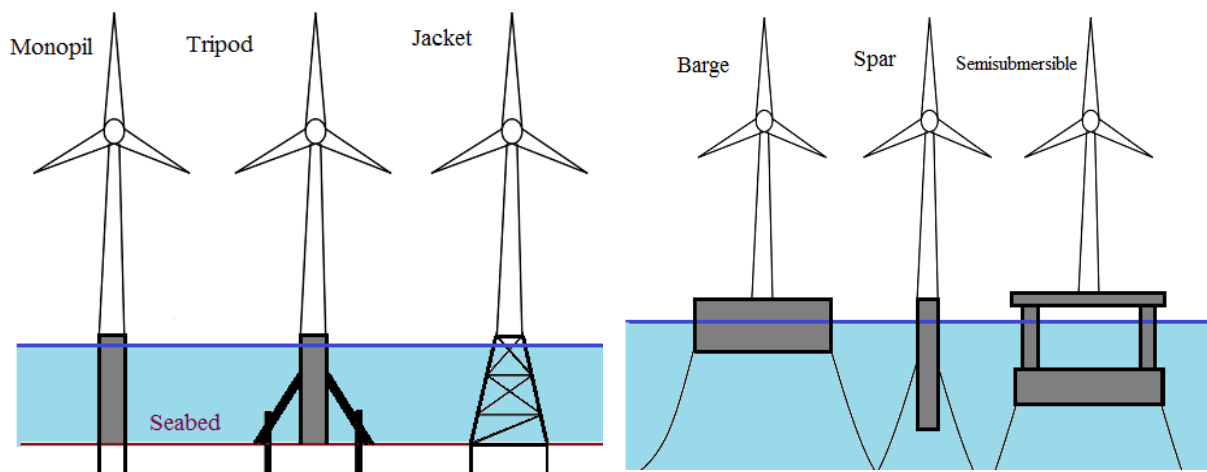


Fig.1: Wind turbine attached to the ground (Karimirad, 2011) Fig.2: Floating wind turbine (Karimirad, 2011)

In recent decades a lot of researchers have modeled offshore floating systems in linear and nonlinear waves (Chandrasekaran et al. 2013; Chandrasekaran and Yuvraj 2013). Perturbation theory has been used for analytical study of these problems (Emmerhoff and Sclavounos 1992). When the order of equation is increased, applying this method becomes extremely complicated. As a result, many numerical solutions for solving these problems have been developed. These numerical solutions mostly have been implemented in simulating waves in a numerical wave tank. Most of efforts done in this field include simulation of the wave itself, constant body and floating bodies with external motions. Koo and Kim simulated a free floating mass in a wave tank using boundary element method in time domain (Koo and Kim 2004). They used Eulerian-Lagrangian method to track free surface. To determine acting force on the floater body, Mode-decomposition method was used. This method is used to find  $\phi_t$  in Bernoli equation. Boo and Kim simulated a cylinder in steady and unsteady waves by employing boundary element and Eulerian-Lagrangian methods in a numerical wave tank (Boo and Kim 1997). They also studied the force exerted on the cylinder from incoming steady and unsteady waves. Ferrant studied a vertical cylinder in numerical wave tank with nonlinear boundary conditions (Ferrant 2001). He used combined wave and current flow for his numerical simulation; he offered his results for incoming waves and wave-current. Celebi et al modeled linear and nonlinear waves in a three dimensional wave tank by Eulerian-Lagrangian and boundary element methods (Celebi et al. 1998). They employed re-meshing and smoothing techniques in Lagrangian section in order to eliminate numerical instability. Grilli et al studied wave breaking numerically by using boundary element and Eulerian-Lagrangian methods (Grilli et al. 2001). Their solution domain was based on a three dimensional wave. Hong and Kim used higher order boundary element method for studying nonlinear waves in a numerical wave tank (Hong and Kim 2000). The system used for simulation was a constant cylinder where exerted force from inlet waves was analyzed. By simulating nonlinear waves, Dommermuth and Yue offered a new solution for tracking free surface and numerical instability (Dommermuth and Yue 1987).

Floating breakwaters (because of extensive capabilities of this type of breakwaters) is used to reduce destructive effects and power of waves at seas. It is possible to install wind turbines on breakwaters by choosing appropriate geometry for them. Installing wind turbines on floating breakwater is worthwhile. Therefore analyzing pressure and determining exerted force would be a great help for designers to choose appropriate geometry for heave plate. For this reason, the purpose of this article is developing a numerical code for simulating breakwaters' performance and the wind turbine erected on them. In this numerical code, prescribed roll motion is analyzed in two dimensions for several geometries with specified length by employing boundary element method and using Euler-Lagrangian method. Typical breakwaters' geometries are selected by studying previous articles. The amount of moment (caused by wave and wind forces) is calculated by applying certain amount of roll on all geometries. The obtained moments show the power, required for a certain displacement. By comparing these moments, stability of different geometries will be specified. On this basis, the appropriate geometry for floating breakwater will be introduced.

## 2. Governing Equations and Numerical Method

Regarding the circumstance of installing breakwaters at sea, which are located with long distance on one direction, it is possible to assume a two dimensional flow.



Fig.3: Schematic view of breakwaters installation(Kwag et al. 2010)

For many hydrodynamics problems, the amount of characteristics velocity and length are much greater than water kinematic viscosity. As a result, viscosity effects compared to inertial effects are negligible. Therefore for proper marine hydrodynamic problems:

$$\text{Incompressible flow} + \text{Inviscid flow} \equiv \text{Ideal current flow}$$

In non-rotational current ( $\nabla \times \mathbf{v} = 0$ ), velocity vector is equal to the gradient of velocity potential and is shown as below:

$$\mathbf{v} = \nabla \phi \tag{1}$$

Combining this equation with Continuity equation for incompressible flows, leads to two dimensional Laplace equations (Becker 1992):

$$\nabla^2 \phi = \frac{\partial^2 \phi}{\partial x^2} + \frac{\partial^2 \phi}{\partial y^2} = 0 \tag{2}$$

Formulating boundary value problem, without determining boundary condition is not complete. Known values are required on domains to determine velocity potential or its derivatives. So, two kinds of boundary conditions are introduced:

- Dirichlet boundary condition  $\Gamma_d(t) \subset \Gamma(t)$ : value of velocity potential on domain is known.
- Neumann boundary condition  $\Gamma_n(t) \subset \Gamma(t)$ : value of normal derivative of velocity potential is known on domain.

Fig. 4 illustrates the fluid's domain and its boundaries for a two-dimensional free floating problem.

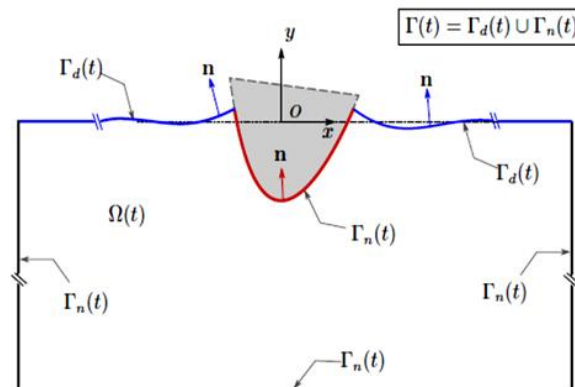


Fig.4: Fluid domain and its solution boundaries (Vinayan 2009)

## 2.1 Boundary element method:

Governing equations in this problem is solved to calculate the pressure magnitude on solid phase boundary and force and moment, exerted on surface of the floater. So, this problem is a boundary value problem; there is no

need to calculate the flow field. Therefore, boundary element method is used as a suitable method for analyzing the flow.

In this method, governing differential equations are converted into integral equations over the boundary or the surface. This means that the boundary will be divided into very small elements and likewise other numerical methods, the problem will be divided into the system of linear algebraic equations which have unique answer. This method can be used easily for simple to complex boundaries. The boundary element method used in this work is based on Isoperimetric Quadratic Elements.

As it is mentioned in the previous section, governing partial differential equation in this problem is Laplace equation (Eq. (2)). Given the boundary conditions,  $\phi$  can be solved by the boundary integral equation:

$$C(P)\phi(P) + \int_{\Gamma} \frac{\partial G(P,Q)}{\partial n} \phi(Q) d\Gamma(Q) = \int_{\Gamma} G(P,Q) \frac{\partial \phi(Q)}{\partial n} d\Gamma(Q) \quad (3)$$

In the above equation,  $\Gamma$  is integral boundary,  $G(p, q)$  is Green function and  $C(P)$  is collision angle at point P. P and Q are source and field points, respectively. The matrix form of Eq. (2) is presented as follows:

$$[A]\phi = [B] \frac{\partial \phi}{\partial n} \quad (4)$$

With determining every single element of matrixes A and B, applying known boundary values, and reordering known value of potential and its derivatives to one side and unknown variables to the other side of the equation, the above system of equations can be solved.. Gauss-Jordan elimination method is used to solve this system of equations.

## 2.2 Nonlinear free surface problem

Free surface problem, known as an initial boundary value problem for a velocity potential, must satisfy the governing Laplace equation. The solution domain includes a numerical wave tank and a floating object with forced motion; it is surrounded by five boundaries.

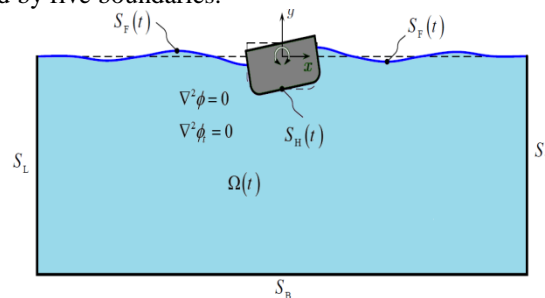


Fig.5: The problem geometry and boundary conditions(Vinayan 2009)

Regarding Fig. 5, boundary conditions are:

1. The left side boundary condition (SL): Newman condition ( $\nabla\phi \cdot n = 0$ )
2. The right side boundary condition (Sw) : Newman condition ( $\nabla\phi \cdot n = 0$ )
3. The down side boundary condition (SB): Newman condition ( $\nabla\phi \cdot n = 0$ )
4. Boundary condition on the free surface (SF(t)): Kinematic and dynamic boundary conditions
5. Boundary condition on the floating body (SH(t)): Newman condition ( $\nabla\phi \cdot n = V(x, t) \cdot n$ )

$V(x, t)$  is the forced motion velocity, applied on the body. The motion is sinusoidal and is limited to roll DOF (Degree of Freedom), so, the equation of motion can be described as the following:

$$\alpha(t) = \alpha_0 \sin(\omega t) \quad (5)$$

$\alpha_0$  and  $\omega$  are respectively amplitude and angular velocity of oscillation. In Cartesian coordinate, velocity of the oscillation is defined as:

$$V(x, t) = (-y\dot{\alpha}, x\dot{\alpha}) \tag{6}$$

The initial conditions of problem at free surface are:

$$\begin{cases} \phi(x, 0) = 0 \\ \eta(x, 0) = 0 \end{cases} \tag{7}$$

### 2.3 Kinematic boundary condition on the free surface

Kinetic boundary condition can be obtained by assuming that fluid cannot pass through the free surface. From Lagrangian viewpoint, for a fluid particle P(x,y) on the free surface, the kinematic boundary condition can be written as (Koo and Kim 2004).

$$\frac{Dx}{Dt} = u = \nabla\phi \Rightarrow \begin{cases} \frac{Dx}{Dt} = u = \phi_x \\ \frac{Dy}{Dt} = v = \phi_y \end{cases} \quad x \in S_F(t) \tag{8}$$

In this equation,  $\frac{D}{Dt} = \frac{\partial}{\partial t} + \nabla\phi \cdot \nabla$  is material derivative from Lagrangian viewpoint and  $u = \nabla\phi = (\phi_x, \phi_y)$  is fluid velocity on the free surface.

### 2.4 Dynamic boundary condition on the free surface

The free surface dynamic boundary condition is achieved from the Bernoulli equation and assuming pressure continuity along the free surface. So, pressure on the free surface should be equal to atmospheric pressure, which results in the general form of the dynamic boundary condition on the free surface:

$$\frac{\partial\phi}{\partial t} + \frac{1}{2}|\nabla\phi|^2 + gy + \frac{P_f}{\rho} = 0 \quad x \in S_F(t) \tag{9}$$

In this equation, g is gravitational acceleration. The conventional form of dynamic free surface boundary condition is defined by pressure in terms of relative pressure. In this case relative pressure at the free surface (Pf) is zero. Eq. (9) is rewritten in Lagrangian form as below:

$$\frac{D\phi}{Dt} = \frac{1}{2}|\nabla\phi|^2 - gy \quad x \in S_F(t) \tag{10}$$

### 2.5 Time evolving of the free surface

To evolve the free surface at time(t + Δt), the Lagrangian form of kinematic and dynamic free surface boundary conditions are integrated with respect to time,

$$\bar{x}^{(k+1)} = \bar{x}^{(k)} + \Delta t (\bar{\nabla}\phi) \quad \bar{x} = (x, y) \tag{11}$$

$$\phi^{(k+1)} = \phi^{(k)} + \Delta t \left( \frac{1}{2}|\nabla\phi^{(k)}|^2 - gy^{(k)} \right) \tag{12}$$

To solve the above equations, numerical Runge-Kutta fourth order method is used. According to the above descriptions, the Lagrangian points and nodes have equal velocity and it should be noted that our view is totally Lagrangian; thus, the nodes along the free surface are elevated along the x and y directions, both.

### 2.6 Smoothing and re-meshing of free surface

At each time step of solving the problem, re-meshing the free surface is needed for maintaining regular intervals between the elements on the free surface. With evolving the free surface at each step, Lagrangian points are transferred to their new position, thereby causing congestion of these points in areas with high gradient and instability of solution. Accordingly, cubic spline method for interpolation of the Lagrangian points on the free surface and redistributing them are used.

Furthermore, for eliminating the sawtooth instability at each time step, Chebyshev five-point smoothing scheme is used. Emerging this type of instability can have either physical or mathematical reasons. One of the primary reasons of this instability is existence of singularity in the corner point of the problem's geometry. This instability first was proposed by Longuet-Higgins and Cokelet(Longuet-Higgins and Cokelet 1976). They used the Chebyshev five-point scheme for eliminating the instability.

### 2.7 Calculating pressure on the floating body

Using Bernoulli equation and assuming non-rotational flow on the free surface, the pressure can be determined.

$$P = -\rho \left( \frac{\partial \phi}{\partial t} + \frac{1}{2} (\nabla \phi)^2 + gy \right) \tag{13}$$

To find out the pressure on the body, calculating  $\phi_t$  in the above equation is fundamental. There are two methods which can be implemented to obtain  $\phi_t$ . The first one is using boundary element method in order to solve  $\phi_t$  instead of  $\phi$  with regard to the known new boundary conditions (Vinayan 2009).

$$C(P)\phi_t(P) + \int_{\Gamma} \frac{\partial G(P,Q)}{\partial n} \phi_t(Q) d\Gamma(Q) = \int_{\Gamma} G(P,Q) \frac{\partial \phi_t(Q)}{\partial n} d\Gamma(Q) \tag{14}$$

New Boundary conditions for solving  $\phi_t$  are:

1. The left side boundary condition: Newman condition ( $\nabla \phi_t \cdot n = 0$ )
2. The right side boundary condition: Newman Condition ( $\nabla \phi_t \cdot n = 0$ )
3. The down side boundary condition: Newman Condition ( $\nabla \phi_t \cdot n = 0$ )
4. Boundary Condition at the free surface: Kinematic and dynamic boundary conditions
5. Boundary Condition on the floating body: Newman Condition ( $\nabla \phi \cdot n = a(x, t) \cdot n$ )

$\Phi$  is acceleration potential and is expressed by the following equation:

$$\Phi = \phi_t + \frac{1}{2} |\nabla \phi|^2 \tag{15}$$

For determining  $\nabla \phi_t \cdot n$  over the body, Tanizawa equations are used (Tanizawa 1995). As the velocity of the body is known, the acceleration of oscillated body can be derived easily. After determination of velocity gradient and wave profile at the free surface, the initial conditions on free surface are obtained from Eq. (10). The second method is using forward finite difference method. In this paper, the former method is used to compute  $\phi_t$ .

### 2.8 Determining the roll moment

Applied moment on the body can be calculated by integrating the pressure equation over its wetted surface.

$$M = \int_{S_B} P(r \times n) ds \tag{16}$$

In eq. (16), M represent the moment,  $n = (n_x, n_y, n_z)$  is normal vector (the positive direction is toward the inside of the floating mass) and  $r = (x, y, z)$  is position vector of a point on the surface.

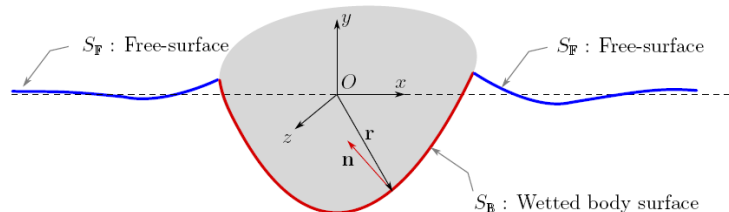


Fig.6. Floating body with normal and position vector(Vinayan 2009)

As the body rotation around roll axis is one degree of freedom, the moment around roll axis can be written as:

$$M_z = - \iint_{S_B} P(xn_y - yn_x) dS \tag{17}$$

## 2.9 Solution algorithm of the numerical code

In the previous sections, the mathematical relations and also the steps which are needed to done to solve the problem are explained. In this section, the simulation method and also the steps to solve the problem are shown in a flowchart. This flowchart is depicted in Fig.7. In this flowchart,  $\phi_n$  is normal component of velocity potential,  $\phi_s$  is tangential component of velocity potential,  $\phi_x$  is horizontal component of velocity potential and  $\phi_y$  is vertical component of velocity potential.

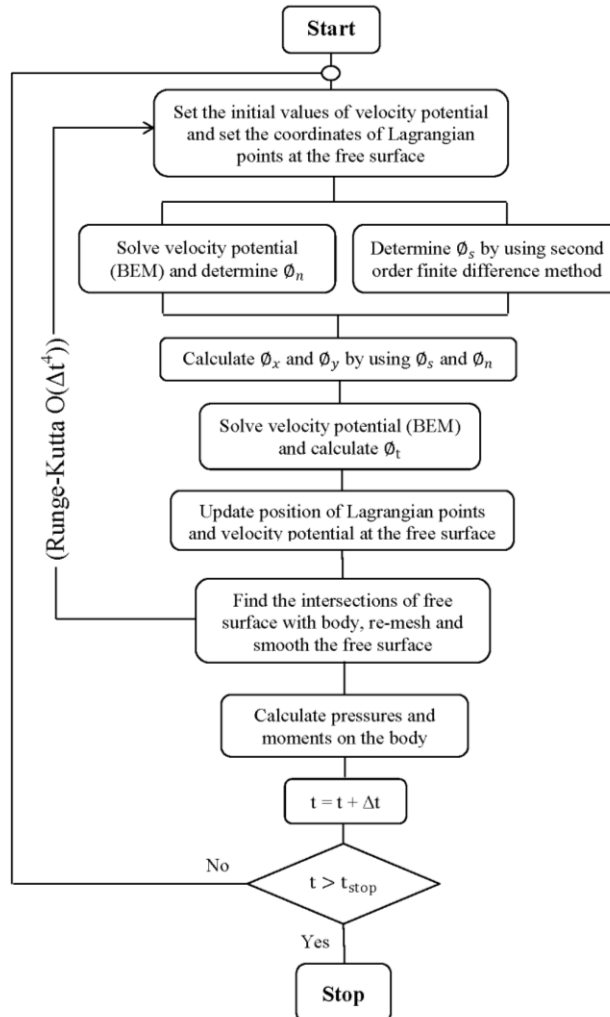


Fig.7. The flowchart which is used to develop the numerical code

## 2.10 Calculating wind force

Beside the moment exerted from wave, the moment applied from wind force is also considerable. The Siemens 5 MW turbine is used for calculation. The cross sectional area of this turbine is about 10500 square meters (Available from: <http://www.4coffshore.com/windfarms/turbine-areva-wind-m5000-116-tid2.html>[cited Feb 24, 2015]). Furthermore, properties of local wind velocity are obtained from the meteorological reports in the Caspian Sea. According to these reports, the density of the air is assumed 1.2 kg/m<sup>3</sup> and averaged wind velocity is 4 m/s (Available from: <http://www.inio.ac.ir/Default.aspx?tabid=2017> [cited Feb 24, 2015]).

For moment calculation related to wind force, first the wind force which is applied on the blades of turbine is obtained from Eq. (18). Then, the moment is calculated from multiplying this force by its related arm.

$$F = \frac{1}{2} \rho A V^2 \quad (18)$$

pis density of air, A is cross sectional area of turbine and V is velocity of wind. In our simulations, cross sectional area is scaled 1:18. So, this area becomes 580 square meters. By substituting the value of the parameters in Eq. (18), the exerted force from wind to the turbine blades is about 5568 N.

### 3. Selected Geometries for Modeling

For numerical modeling and evaluation, various geometries of breakwaters are chosen on the basis of the previous studies (Fig. 8).

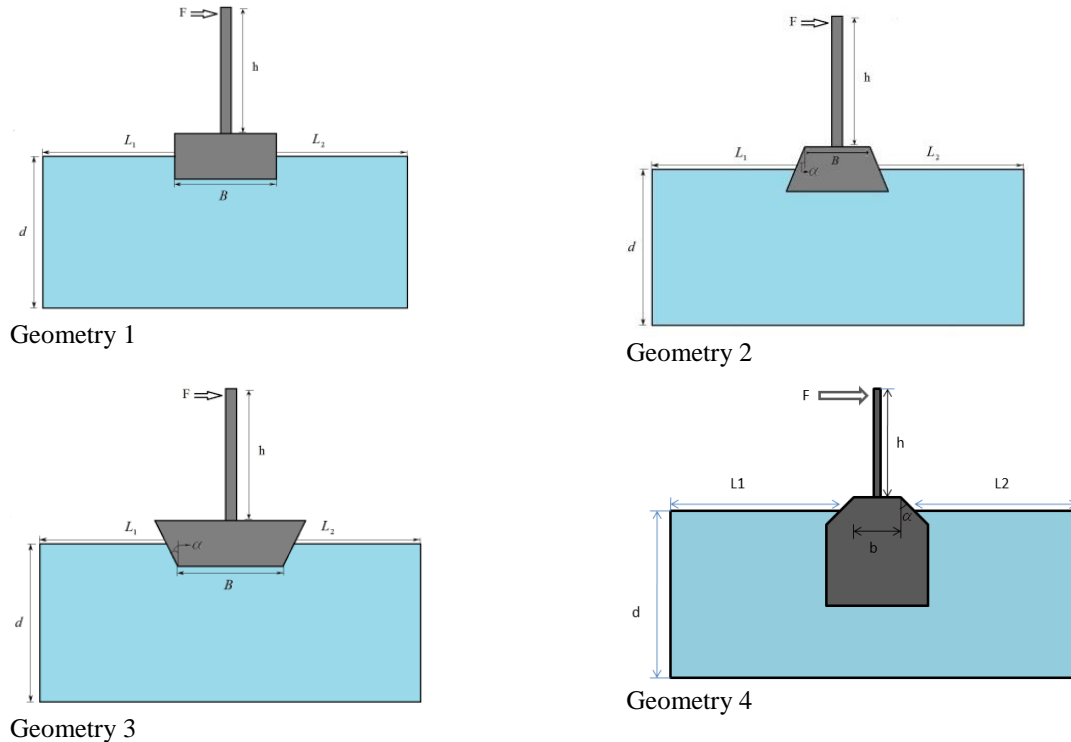


Fig.8: Selected geometries for simulation

Table 1 shows the characteristics of the selected geometries. With regard to the scale of model, height of all geometries is equal to 2 meters. The scale analysis on this research is based on the Froude similarity. The concept and also the relations of this scale analysis are comprehensively explained on the reference (Kelly 2007). The Angle  $\alpha$  differs for different geometries and is mentioned for each geometry in the next section.

Table 1: Dimensions of geometries of Fig. 8

$B(m)$	$L_1(m)$	$L_2(m)$	$d(m)$	$h(m)$
1	20	20	5	5

### 5. Results and Discussion

In order to simulate the problem, a numerical code is developed based on boundary element method using MATLAB Software. For validation, the result from solution of boundary element method is compared with the result of analytical solution of the piston wave-maker (Fig. 9) (Tanizawa 2000). Analytical solution for wave potential and wave profile of a piston type wave maker are expressed by the following equations:

$$\phi(x, y, t) = \frac{4s \tanh kh \sinh kh}{\omega(2kh + \sinh 2kh)} \cdot [\cosh(y + h) \cos(kx - \omega t)] \quad (19)$$



$$\eta(x, t) = \frac{4s \sinh^2 kh}{2kh + \sinh 2kh} \sin(kx - \omega t) \quad (20)$$

In Equations (19) and (20),  $s$  is the amplitude of piston motion,  $\omega$  is motion frequency,  $h$  is water depth and  $k$  is wave number. Results for wave profiles from  $t = 0$  to  $t = 4T$  for both boundary element and analytical methods are compared which is presented in Fig. 8. The history of wave profile is plotted for the distance of  $x = 5\text{m}$  from the wave maker's piston. It can be seen that both models are in good agreement and they produce identical results.

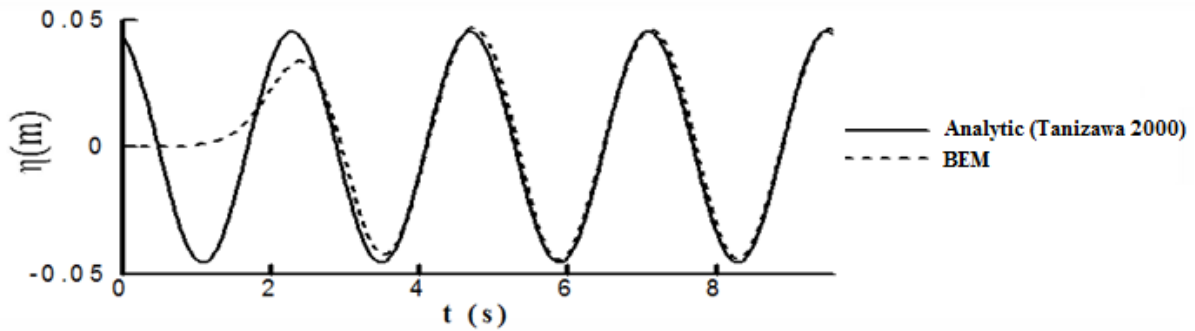


Fig.9: Comparison of analytical solution and numerical solution of the boundary element method at  $T = 2.4\text{ s}$  and  $A = 0.1$

In the previous section, selected geometries of breakwaters are introduced and explained. As mentioned before, these geometries had been selected with the purpose of using as a breakwater and installation of offshore wind turbines. Applying these multifunctional breakwaters at sea has some difficulties. The most important one is stability of structure against waves. In this work, the moment applied on the body of floating breakwaters and the wave profile next to the left and right side of body are obtained by simulating the motion of selected geometries.

As these floating bodies have prescribed roll motion, to achieve a mutual standard for better comparison, body oscillation for all geometries was kept the same. Therefore, in final assessment it was assumed that whatever the moment is bigger for achieving this amount of oscillation, that geometry of floating breakwater is more stable against waves. Another point that can verify this assumption is the power of waves applied to the floaters body. By obtaining wave profiles next to these geometries and by considering that a more stable geometry demands a stronger wave with larger wave amplitude for reaching a predetermined oscillation, stability of these breakwaters can be evaluated.

With regard to validation of our numerical code, results of various breakwater geometries with prescribed Roll motion are given. The results are for the wave profile at free surface and moment on body surface. In these results variation in breakwater geometries are considered. It is assumed that the amplitude of body oscillation ( $\alpha_0$ ) and Froude number which is given by Equation (21) are 0.4, both.

$$Fr = \omega \sqrt{\frac{B}{2g}} \quad (21)$$

In Eq. (21),  $\omega$  is oscillation frequency of the breakwater and  $B$  is breakwater width. Regarding geometries in Fig. 8 and their dimensions in table 1, the moment applied on floating body and the wave profile next to the left and right side of the floater are calculated.

Fig. 10 illustrates that geometry 2 has the maximum amount of moment and geometry 3 has the minimum amount. The results indicate that increasing the angle, leads to enhance in the amount of moment. As floaters have prescribed roll motion and they have identical oscillation, the more moment they need to oscillate the more stable they are. This shows that geometry 2 has more stability and it is more appropriate to be considered as geometry of floating breakwater.

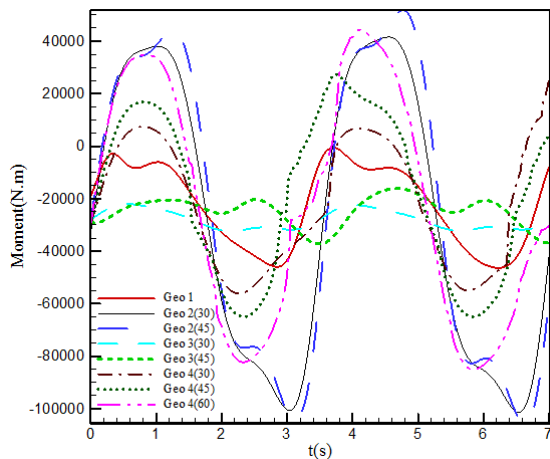


Fig.10: Moment applied on floating breakwater body

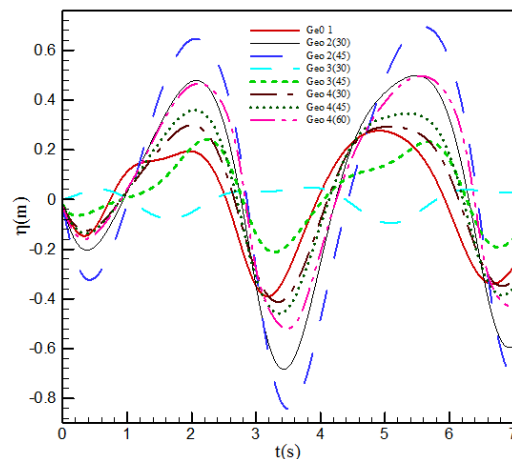


Fig.11: Wave profile next to the left side of breakwater body

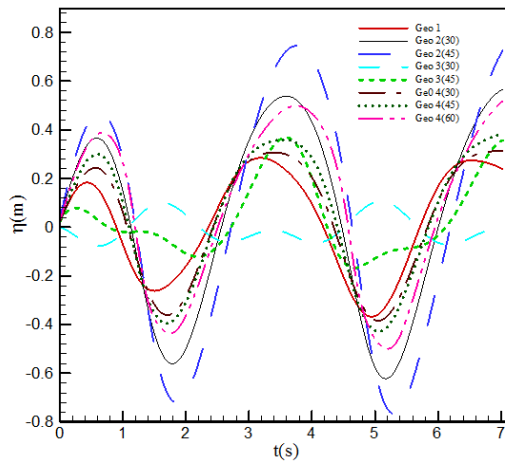


Fig.12: Wave profile next to the right side of breakwater body

Figs. 11 and 12 confirm the mentioned conclusion. It can be seen from these figures that in geometry 2, stronger waves with bigger amplitude are needed for the same body oscillation. So, geometry 2 is more stable. Also increasing angle  $\alpha$  improves stability. In simulated geometries, geometry 2 with 45 degree angle has the most stability and thus it is more suitable for a floating breakwater.

#### 4. Conclusions

In this paper, by analyzing and comparing moments produced by incoming waves and wave profile next to the right and left side of breakwater body, a suitable geometry of breakwater is introduced for multifunctional usage. In this study, the boundary element method is used to solve governing equations by assuming the potential flow. Also, the combined Eulerian-Lagrangian method is used to solve numerical parameters on the boundaries in order to analyze pressure, force and other hydrodynamics parameters on the surface of the floating body and to promote the free surface in each time step. Simulation results for prescribed roll motion in different breakwater geometries show that geometries 2 and 3 need maximum and minimum amounts of moment for a same amount of oscillation, respectively. Also, the results depict that increasing the angle of body increase this amount. Also, wave profiles next to the left and right side of the body are obtained. According to the results, for geometry 2, stronger wave with bigger amplitude is needed for the same body oscillation. With regard to the results, geometry 2 with angle 45 degree has the maximum stability and therefore it is the most suitable one to be used as the breakwater geometry.

## References

- Becker, A. A. (1992): The boundary element method in engineering: a complete course, McGraw-Hill London.
- Boo, S. and Kim, C. (1997): Nonlinear irregular waves and forces on truncated vertical cylinder in a numerical wave tank, Proceedings of the 7th International Offshore and Polar Engineering Conference, ISOPE, Honolulu, HI. pp. 76-84.
- Celebl, M., Kim, M. and Beck, R. (1998): Fully nonlinear 3-D numerical wave tank simulation, Journal of Ship Research, vol.42, No. 1, pp. 33-45.
- Chandrasekaran, S., Kumar, D. and Ramanathan, R. (2013): Dynamic response of tension leg platform with tuned mass dampers, Journal of Naval Architecture and Marine Engineering, vol.10, no. 2, pp.149-156. <http://dx.doi.org/10.3329/jname.v10.i2.16184>
- Chandrasekaran, S. and Yuvraj, K. (2013): Dynamic analysis of a tension leg platform under extreme waves, Journal of Naval Architecture and Marine Engineering, vol.10, no. 1, pp. 59-68. <http://dx.doi.org/10.3329/jname.v10i1.14518>
- Dommermuth, D.G. and Yue, D.K. (1987): Numerical simulations of nonlinear axisymmetric flows with a free surface, Journal of Fluid Mechanics, vol. 178, pp.195-219. <http://dx.doi.org/10.1017/S0022112087001186>
- Emmerhoff OJ, Sclavounos P (1992) The slow-drift motion of arrays of vertical cylinders, Journal of fluid mechanics, vol. 242, pp. 31-50. <http://dx.doi.org/10.1017/S002211209200226X>
- Ferrant, P. (2001): Runup on a cylinder due to waves and current: potential flow solution with fully nonlinear boundary conditions, International Journal of Offshore and Polar Engineering, vol.11, no. 1, pp.33-41.
- Fulton, G., Malcolm, D., Elwany, H., Stewart, W., Moroz, E., Dempster, H. (2007):Semi-Submersible Platform and Anchor Foundation Systems for Wind Turbine Support: August 30, 2004-May 31, 2005, National Renewable Energy Laboratory, 2007.
- Grilli, S.T., Guyenne, P., Dias, F. (2001): A fully non-linear model for three-dimensional overturning waves over an arbitrary bottom, International Journal for Numerical Methods in Fluids, vol.35, no. 7, pp.829-867. [http://dx.doi.org/10.1002/1097-0363\(20010415\)35:7%3C829::AID-FLD115%3E3.0.CO;2-2](http://dx.doi.org/10.1002/1097-0363(20010415)35:7%3C829::AID-FLD115%3E3.0.CO;2-2)
- Hong, S.Y., Kim, M. (2000): Nonlinear wave forces on a stationary vertical cylinder by HOBEM-NWT, Intl. Conf. ISOPE'00, pp. 214-220. <http://www.4coffshore.com/windfarms/turbine-areva-wind-m5000-116-tid2.html>, Turbine Areva Wind M5000-116, Accessed on 24 Feb. 2015. <http://www.inio.ac.ir/Default.aspx?tabid=2017>, Iran National Institute for Oceanography and Atmospheric Science, Accessed on 24 Feb. 2015.
- Karimirad, M. (2011): Stochastic dynamic response analysis of spar-type wind turbines with catenary or taut mooring systems, Ph.D. thesis, Norwegian University of Science and Technology, Doctoral theses at NTNU, 2011:8, Trondheim, Norway.
- Kelly, S. J. (2007): Hydrodynamic optimisation of point wave-energy converter using laboratory experiments, Civil Engineering, University of Auckland,
- Koo, W., Kim, M. H. (2004): Freely floating-body simulation by a 2D fully nonlinear numerical wave tank, Ocean Engineering, vol. 31, no. 16, pp.2011-2046. <http://dx.doi.org/10.1016/j.oceaneng.2004.05.003>
- Kwag, D. J., Cho, I. H., Bang, S., Cho, Y. (2010): Embedded Suction Anchors for Mooring of a Floating Breakwater, Journal of Offshore Mechanics and Arctic Engineering, vol.132, no. 2, pp.021603-021603. <http://dx.doi.org/10.1115/OMAE2008-57055>
- Longuet-Higgins, M. S., Cokelet, E. (1976): The deformation of steep surface waves on water. I. A numerical method of computation. Proceedings of the Royal Society of London, A. Mathematical and Physical Sciences, vol. 350, no. 1660, pp.1-26. <http://dx.doi.org/10.1098/rspa.1976.0092>
- Mostafa, N., Murai, M., Nishimura, R., Fujita, O. and Nihei, Y. (2012): Study of motion of spar-type floating wind turbines in waves with effect of gyro moment at inclination, Journal of Naval Architecture and Marine Engineering, vol.9, no. 1, pp.67-79. <http://dx.doi.org/10.3329/jname.v9i1.10732>
- Tanizawa, K. (1995): A nonlinear simulation method of 3-D body motions in waves (1st Report). Journal of Society of Naval Architect of Japan, vol. 178, no.178, pp.179-191.
- Tanizawa, K. (2000): The state of the art on numerical wave tank, Proc. 4th Osaka colloquium on seakeeping performance of ships, pp 95-114. [http://dx.doi.org/10.2534/jjasnaoe1968.1995.178\\_179](http://dx.doi.org/10.2534/jjasnaoe1968.1995.178_179)
- Vinayan, V. (2009): A Boundary Element Method for the strongly nonlinear analysis of ventilating water-entry and wave-body interaction problems, UT-OE Rep. 09-2, Ocean Engineering Group, Department of Civil Engineering, Architectural and Environmental Engineering, University of Texas at Austin, Austin, TX, 2009.
- Withee, J. E. (2004): Fully coupled dynamic analysis of a floating wind turbine system, Monterey, California. Naval Postgraduate School.